HHS Public Access

Author manuscript

Immunity. Author manuscript; available in PMC 2013 December 14.

Published in final edited form as:

Immunity. 2012 December 14; 37(6): 1037–1049. doi:10.1016/j.immuni.2012.08.017.

Reactive oxygen species (ROS)-induced actin glutathionylation controls actin dynamics in neutrophils

Jiro Sakai[1,#], **Jingyu Li**[1,2,#], **Kulandayan K. Subramanian**[1,#], **Subhanjan Mondal**[1], **Besnik Bajrami**[1], **Hidenori Hattori**[1], **Yonghui Jia**[1], **Bryan C. Dickinson**[4], **Jia Zhong**[1], **Keqiang Ye**[3], **Christopher J Chang**[4], **Ye-Shih Ho**[5], **Jun Zhou**[2], and **Hongbo R. Luo**[1,*]

[1]Department of Pathology, Harvard Medical School; Department of Lab Medicine, Children's Hospital Boston; Dana-Farber/Harvard Cancer Center

[2]Jun Zhou, Department of Genetics and Cell Biology, Tianjin Key Laboratory of Protein Science, College of Life Sciences, Nankai University, Tianjin, China

[3]Department of Pathology and Laboratory Medicine, Emory University School of Medicine, Atlanta, GA, USA

[4]University of California at Berkeley, Department of Chemistry and the Howard Hughes Medical Institute, Berkeley, CA

[5]Institute of Environmental Health Sciences and Department of Biochemistry and Molecular Biology, Wayne State University, Detroit, MI

Summary

The regulation of actin dynamics is pivotal for cellular processes such as cell adhesion, migration, and phagocytosis, and thus is crucial for neutrophils to fulfill their roles in innate immunity. Many factors have been implicated in signal-induced actin polymerization, however the essential nature of the potential negative modulators are still poorly understood. Here we report that NADPH oxidase-dependent physiologically generated reactive oxygen species (ROS) negatively regulate actin polymerization in stimulated neutrophils via driving reversible actin glutathionylation. Disruption of glutaredoxin 1 (Grx1), an enzyme that catalyzes actin deglutathionylation, increased actin glutathionylation, attenuated actin polymerization, and consequently impaired neutrophil polarization, chemotaxis, adhesion, and phagocytosis. Consistently, Grx1-deficient murine neutrophils showed impaired *in vivo* recruitment to sites of inflammation and reduced bactericidal

[*]To whom all correspondence should be addressed. Enders Research Building, Room 811, Boston, MA 02115, USA, Hongbo.Luo@childrens.harvard.edu, Phone: 617-919-2303, Fax: 617-730-0885.
[#]These authors contributed equally to this work.

Author Contributions

Jiro Sakai, Jingyu Li, and Kulandayan Subramanian designed and carried out experiments, analyzed data and prepared manuscript. Besnik Bajrami, Subhanjan Mondal, Hidenori Hattori, Yonghui Jia, Keqiang Ye and Jun Zhou helped with designing experiments, analyzing data and evaluating manuscript. Jia Zhong bred mice. Bryan C. Dickinson and Christopher J. Chang synthesized and provided PF6-AM, Ye-Shih Ho provided the *Grx1*$^{-/-}$ mice. Hongbo R. Luo designed experiments, analyzed data, and wrote paper.

capability. Together, these results present a physiological role for glutaredoxin and ROS- induced reversible actin glutathionylation in regulation of actin dynamics in neutrophils.

Introduction

During phagocytosis or upon chemoattractant stimulation, phagocytes release a large amount of reactive oxygen species (ROS), a process known as "respiratory burst" or "oxidative burst" (Subramanian and Luo, 2009). These ROS are mainly produced by phagocytic NADPH oxidase (a.k.a. NOX2 complex). Insufficient activation of the oxidase, as in chronic granulomatous disease (CGD), leads to inadequate elimination of pathogens and causes severe, life threatening infections (Dinauer, 2005). Although classically the function of “respiratory burst” is to aid in the capability of phagocytes to kill pathogens, more recent studies have shed new light on unconventional roles for ROS and NADPH oxidase activation in cellular signal transduction and functionality (Dickinson and Chang, 2011; Subramanian and Luo, 2009). Redox regulation of cell signaling often involves modification of reactive thiols on specific cysteine residues of proteins, converting them from a reduced to an oxidized form. The major types of thiol modifications that have been shown to play an important redox dependent role include glutathionylation, sulfenic acid formation, nitrosylation and disulfide bond formation (Ghezzi, 2005; Hurd et al., 2005; Janssen-Heininger et al., 2008; Shelton et al., 2005).

In several cell types, ROS production has been shown to drive the glutathionylation of free thiol groups (-SH) on cysteine residues of proteins to form Protein-glutathione mixed disufide adducts (Pr-SSG) (Gallogly and Mieyal, 2007; Ghezzi, 2005; Hurd et al., 2005; Janssen-Heininger et al., 2008; Leichert and Jakob, 2006; Ying et al., 2007). Protein S-glutathionylation can affect the function of various proteins including actin, protein tyrosine kinases and phosphatases, Ras, and transcription factors such as NF-κB, and hence modulate cell signaling and function. Glutathionylation of a critical cysteine, Cys374, in actin, has been shown to reduce the ability of G-actin to polymerize into F-actin polymers (Dalle-Donne et al., 2003; Lassing et al., 2007; Shelton et al., 2005; Wang et al., 2001). Nevertheless, whether actin glutathionylation is critical for any actin-mediated cellular processes under physiological condition is unknown.

The regulation of actin dynamics is pivotal for a variety of cellular processes such as cell adhesion, migration, and phagocytosis, and thus is crucial for neutrophils to fulfill their roles in innate immunity. In this study, we identified NADPH oxidase dependent ROS as physiological regulators of pseudopod formation and chemotactic migration in neutrophils. ROS regulated neutrophil chemotaxis by directly modulating actin glutathionylation and polymerization. We further showed that the dynamic actin glutathionylation in neutrophils could be regulated by glutaredoxin 1 (Grx1), a cytosolic thiol disulfide oxido-reductase (thioltransferase) that mediates protein deglutathionylation. Disruption of Grx1 resulted in elevated actin glutathionylation and attenuated actin polymerization, leading to impaired neutrophil polarization, chemotaxis, adhesion, and phagocytosis. These results establish ROS-induced actin glutathionylation and its modulation by glutaredoxin as key physiological regulatory mechanisms controlling actin dynamics in neutrophils.

Results

NADPH oxidase-mediated ROS production leads to elevated actin glutathionylation in chemoattractant-stimulated neutrophils

Neutrophils release a large amount of ROS in response to chemoattractant stimulation. To examine the role of ROS-induced glutathionylation in neutrophil chemotactic signaling, we first explored protein glutathionylation using a glutathione specific antibody. A major band corresponding to the size of actin (42 kDa) was detected in fMLF stimulated neutrophil lysates (Figure 1A and Figure S1). Treatment with dithiothreitol (DTT) caused a decrease of signal, consistent with the reduction of glutathione mixed disulfides (Figure 1B). In order to confirm that the major glutathionylated protein was actin, a membrane permeant biotinylated glutathione ester (BioGEE) was used to detect glutathionylated proteins in neutrophils. Lysates of BioGEE treated, fMLF stimulated neutrophils were pulled-down with either Streptavidin-agarose or an actin antibody, and then probed with actin antibody and Streptavidin-HRP, respectively. Both approaches clearly demonstrated that actin was indeed a major glutathionylated protein in fMLF stimulated neutrophils (Figure 1C–D).

ROS are mainly produced by NADPH oxidase in chemoattractant-stimulated neutrophils. We next examined whether NADPH oxidase-dependent ROS production is required for the actin glutathionylation. Chemoattractant stimulation elicited nearly a three-fold increase in actin glutathionylation in 5 min. Treatment with diphenyleneiodonium chloride (DPI), a well-characterized flavoprotein inhibitor that is known to suppress the activity of NADPH oxidase, resulted in a significant decrease of actin glutathionylation, before and after chemoattractant stimulation (Figure 1E). We detected a small increase in actin glutathionylation at the 5 min time point in DPI treated neutrophils. This was most likely caused by the residual NADPH oxidase activity left in these cells.

We next measured chemoattractant-elicited actin glutathionylation using a CGD mouse in which the gp91 subunit of NADPH oxidase holoenzyme was deleted (Pollock et al., 1995). fMLF-stimulated WT neutrophils displayed maximal glutathionylation at 5 min after stimulation. In contrast, CGD neutrophils only showed background actin glutathionylation, 5 min after fMLF stimulation (Figure 1F). These results clearly show that NADPH oxidase-dependent ROS production promotes actin glutathionylation in stimulated neutrophils. It is noteworthy that as in many other cell types, ROS can be produced by other mechanisms (e.g. mitochondria). ROS still exist in DPI-treated and CGD neutrophils. Consequently, basal actin glutathionylation was detected even before chemoattractant stimulation and NADPH activation.

ROS production and protein glutathionylation occur in the leading edge of chemotaxing neutrophils, colocalizing with actin

To further study the physiological role of ROS-induced actin glutathionylation, we examined the subcellular localization of ROS production and glutathionylation during neutrophil chemotaxis, a process driven by actin polymerization. We determined the localization of ROS in migrating neutrophils using a cell permeant indicator for ROS, 5-(and-6)-carboxy-2′,7′-dichlorodihydrofluorescein diacetate (carboxy-H2DCFDA). In

unstimulated neutrophils the ROS dye displayed a uniform distribution throughout the cytosol. As the neutrophils started polarizing and chemotaxing towards the source of chemoattractant, the probe intensely localized at the pseudopods that were generated at the front of the cell (Movie S1). This localized accumulation of ROS was completely abolished in either DPI-treated human neutrophils (Figure 2A–B, Movie S2), or CGD mouse neutrophils (Figure 2C–D), confirming that this cellular event was dependent on the activation of NADPH oxidase complex.

Activated NADPH oxidase complex catalyzes the conversion of molecular oxygen to superoxide (O^{-}_{2}), from which various ROS such as H_2O_2, OH^{-}, HOCl and ONOO- are synthesized and released to the extracellular space and phagocytic vacuoles. Among these ROS, only H_2O_2 is membrane permeable and can possibly travel to the cytosolic space to modulate actin function (Miller et al., 2010). Traditional methods for ROS detection, such as the carboxy-H2DCFDA method used above, suffer from nonspecific reactivity with all ROS. In order to examine intracellular localization of H_2O_2, we used Peroxyfluor-6 acetoxymethyl ester (PF6-AM), a new chemoselective fluorescent indicator for H_2O_2 with improved sensitivity. This fluorescent probe features a boronate chemical switch that allows for selective detection of H_2O_2 over other ROS, combined with acetoxymethyl ester–protected phenol and carboxylic acid groups for enhanced cellular retention and sensitivity (Dickinson et al., 2011) (Figure 2E). Similar to the carboxy-H2DCFDA staining, H_2O_2 production, monitored by PF6-AM fluorescence, was highly localized at the front of the chemotaxing cells (Figure 2F–G, Movies S3–4).

Next, we determined the spatial distribution of protein glutathionylation in polarized migrating neutrophils (Figure S2). We found that protein glutathionylation was localized in the front of polarized neutrophils and colocalized with actin staining (Figure 2H). Addition of reducing agent, DTT, to the immunostaining protocol completely inhibited the glutathionylated protein localization at the front of the cell, but preserved the actin staining at the cell periphery (Figure 2I). Similar results were obtained when free glutathione (GSH) was added to the primary antibody mix, confirming that the protein glutathionylation staining was specific (Figure 2J). Consistent with the western blotting results, treatment with DPI reduced actin glutathionylation (Figure 2K). Similarly, basal protein glutathionylation was still detected in DPI-treated neutrophils. However, compared to untreated cells, glutathionylation staining was more diffuse and not always restricted to pseudopodia in DPI-treated neutrophils.

ROS depletion leads to significantly higher amount of F-actin

Since NADPH oxidase-mediated ROS production and protein glutathionylation were localized at the sites of intense actin polymerization in polarized neutrophils, we next investigated whether ROS production can affect chemoattractant-elicited actin polymerization. Neutrophils treated with DPI always showed significantly higher F-actin amounts compared to untreated neutrophils. F-actin amounts were increased both before (0 sec) and after fMLF stimulation (at 30 sec and 3 min) (Figure 3A). A similar result was observed in CGD mouse neutrophils (Figure 3B). It is noteworthy that actin polymerization and depolymerization are dynamic processes that occur in both fMLF stimulated and

unstimulated neutrophils. A large amount of glutathionylated actin was also detected in unstimulated neutrophils (Figure 1E–F), suggesting that this actin modification might also be involved in regulating F-actin concentration in these "quiescent" neutrophils. Consistently, we observed enhanced F-actin amounts in DPI-treated WT or CGD neutrophils even at times 0 and 1 min before the ROS concentration reaches the peak value (Figure 3). However, consistent with the dramatic elevation of actin glutathionylation at the 5 min time point, we observed the most significant increase of F-actin in DPI-treated WT or CGD neutrophils 5 min after chemoattractant stimulation (Figure 3).

Reducing actin glutathionylation by over-expressing glutaredoxin leads to increased F-actin, formation of multiple pseudopods, and defective chemotaxis

Protein glutathionylation is a dynamic reversible process (Dalle-Donne et al., 2003). Deglutathionylation is mainly catalyzed by glutaredoxin (Grx), a thiol disulfide oxido-reductase (thioltransferase) (Subramanian and Luo, 2009; Wang et al., 2001) (Figure 4A). Mammalian cells express 2 dithiol Grx isoforms, Grx1 and Grx2. Grx1 is a cytosolic protein, whereas Grx2 is in mitochondria (Meyer et al., 2009). Actin glutathionylation is a cytosolic event and is mainly regulated by Grx1. Disruption of Grx1 is sufficient to increase protein glutathionylation in mouse embryonic fibroblast (MEF) cells, Lens Epithelial cells (LEC), and the lungs (Aesif et al., 2011; Chung et al., 2010; Ho et al., 2007; Lofgren et al., 2008). To further investigate the role of actin glutathionylation in neutrophil chemotaxis, we suppressed actin glutathionylation by overexpressing Grx1 in neutrophil-like differentiated HL60 cell (dHL60), a model system for studying neutrophil chemotaxis (Figure 4B). Grx1 overexpression significantly reduced actin glutathionylation (Figure 4C). Consistent with the most drastic elevation of actin glutathionylation at the 5 min time point, a significant increase in F-actin in Grx1 overexpressing neutrophils was observed 5 min after chemoattractant stimulation (Figure 4D). In wild-type cells, the amount of F-actin went back to the basal concentration at this time point. In contrast, more than half of the chemoattractant-elicited F-actin remained in Grx1 overexpressing cells. As a result, the Grx1 overexpressing cells displayed defective chemotactic migration (Figure 4E). To take a closer look at the morphological changes elicited by Grx1 overexpression, multiple pseudopod formation was measured in chemotaxing neutrophils. We observed that Grx1 overexpressing cells showed multiple pseudopodia much more frequently compared to control cells (Figure 4F). These defects caused by Grx1 overexpression are similar to what were observed in neutrophils depleted of ROS (Hattori et al., 2010), in which actin glutathionylation was also reduced (Figure 1).

A recent study has suggested that actin glutathionylation occurs via a sulfenic acid intermediary (Johansson and Lundberg, 2007). Accordingly, we tested if sodium arsenite (Kim et al., 2002; Saurin et al., 2004), a reducing agent that specifically converts sulfenic acids to thiols, could block actin glutathionylation and impair neutrophil chemotaxis. Similar to the DPI treatment and Grx1 overexpression, sodium arsenite could also significantly decrease actin glutathionylation in neutrophils (Figure 4G), suggesting that actin glutathionylation does occur via a sulfenic acid intermediary. As a result, arsenite treatment led to formation of multiple pseudopodia and impaired neutrophil chemotaxis (Figure 4H and Movie S5). Collectively, these results demonstrated that actin glutathionylation plays a

critical role in neutrophil chemotaxis. Reduction of actin glutathionylation leads to increased F-actin, formation of multiple pseudopods, and defective chemotaxis. These results are also consistent with the critical role of ROS in chemotaxis. Although we cannot completely rule out the possibility that different chemoattractant may trigger different chemotactic signaling pathway, it seems there is a correlation between ROS production and migration efficiency. We tested G-CSF and TNFa, the two cytokines that don't induce significant ROS production. Interestingly, neither of them are good chemoattractants. In our chemotaxis device, neutrophil didn't migrate in G-CSF or TNFa gradient (Figure S3).

Elevating actin glutathionylation by disrupting glutaredoxin rescues neutrophil chemotaxis defects induced by ROS depletion

Our previous study showed that depletion of ROS led to formation of multiple pseudopods and defective chemotaxis (Hattori et al., 2010). We hypothesize that these chemotaxis defects are mediated by reduced actin glutathionylation and defective actin depolymerization. To test this hypothesis, we examined whether these defects can be rescued by elevating actin glutathionylation via Grx1 inhibition. It was reported that Cd^{2+}, a known glutaredoxin inhibitor (Chrestensen et al., 2000), inhibits intracellular actin deglutathionylation and thus increases the amount of glutathionylated actin (Wang et al., 2001). Accordingly, we investigated the effect of Cd^{2+} on neutrophil chemotaxis and found that Cd^{2+} treatment could elevate actin glutathionylation in neutrophils (Figure 5A). Co-treatment with Cd^{2+} significantly improved the directional migration efficiency of DPI-treated neutrophils (Figure 5B). Since the effect of Cd^{2+} may not be specific, to definitively prove the role of actin glutathionylation and glutaredoxin in neutrophil chemotaxis, we silenced the expression of Grx1 using siRNA (Figure 5C). Differentiated neutrophil like HL60 (dHL60) cells depleted of Grx1 showed much increased amount of glutathionylated actin (Figure 5D). Similar to Cd^{2+} treatment, siRNA silencing of Grx1 significantly improved the directional migration efficiency of DPI-treated dHL60 cells, further demonstrating that ROS-mediated actin glutathionylation plays a critical role in neutrophil chemotaxis (Figure 5E). To demonstrate that the chemotaxis defects elicited by ROS depletion are mediated by impaired actin depolymerization, we examined whether these defects can be rescued by elevating actin depolymerization by latrunculin B which binds actin monomers near the nucleotide binding cleft and prevents them from polymerizing. As expected. due to reduced actin polymerization, the migration speed of neutrophils was reduced by latrunculin treatment. However, ROS depletion-induced formation of multiple pseudopodia and impaired directional migration could be rescued, indicating that the chemotaxis defects are at least partially mediated by actin (Figure 5F).

Previous studies revealed that ROS-elicited actin glutathionylation occurs on Cys374 at the C-terminal of the protein (Dalle-Donne et al., 2003; Lassing et al., 2007; Shelton et al., 2005; Wang et al., 2001). To further explore the role of actin glutathionylation in ROS mediated chemotactic signaling, we transduced HL60 cells with constructs expressing either wild-type actin or mutant forms of actin that cannot be glutathionylated (Figure 5G). In dHL60 cells, only wild-type EGFP-actin (Cys^{374}) displayed increased glutathionylation upon fMLF stimulation. Consistent with the previous studies, mutation of the Cys^{374} to Ala, Glu or Asp abolished chemoattractant-elicited actin glutathionylation (Figure 5H). dHL60

cells overexpressing wild-type EGFP-actin showed normal chemotactic migration. In contrast, dHL60 cells overexpressing mutant forms of actin displayed impaired directional migration, and showed multiple pseudopodia much more frequently compared to cells expressing wild-type EGFP-actin (Figure 5I). These effects were not due to alteration of the net charge at the exposed C-terminal tail, since cells expressing Ala^{374} (neutral) behaved similarly to cells expressing Glu^{374} or Asp^{374} (negatively charged). Moreover, it was previously reported that substitution of Cys^{374} with Ala does not affect actin polymerization in conditions unrelated to ROS, suggesting that Cys^{374} is not critical for actin polymerization *per se* (Tsapara et al., 1999). Thus, the defective chemotaxis of the cells expressing mutant forms of actin was most likely caused by impaired ROS-induced actin glutathionylation. Considering that the endogenous wild-type actin still exist in dHL60 cells overexpressing mutant forms of actin, these results also suggest that the mutant forms had a dominant-negative effect in regulating actin dynamics during neutrophil chemotaxis. The observed chemotaxis defect and multiple pseudopodia formation were most likely caused by impaired depolymerization of the mutant actin in "old" pseudopod, instead of lack of functional G-actin for the formation of "new" pseudopod. Taken together, our results demonstrate that ROS-induced actin glutathionylation is a key regulatory mechanism for efficient neutrophil chemotactic migration.

Grx1 is a key physiological regulator of actin dynamics in neutrophils

The results described above suggest that Grx1 is a positive regulator of actin polymerization. It drives the cycle of actin glutathionylation and deglutathionylation. To test whether Grx1 is directly involved in neutrophil chemotaxis in vivo, we used a *Grx1*$^{-/-}$ mouse (Ho et al., 2007) in which Grx1 protein expression was completely abolished (Figure 6A). Grx1 deficient mice were similar to their WT littermates in body weight, survival rate, appearance, and behavior. The differential leukocyte counts in bone marrow and peripheral blood were also normal. In addition, Grx1 deficient neutrophils produced the same amount of ROS in response to chemoattractant or phorbol-12-myristate-13-acetate (PMA) stimulation compared to WT neutrophils (Figure S4). Grx1 deficiency enhanced chemoattractant-elicited actin glutathionylation (Figure 6B) and suppressed actin polymerization (Figure 6C). We next examined chemotaxis of WT and *Grx1*$^{-/-}$ neutrophils using a EZ-Taxiscan chemotaxis device in which a stable chemoattractant gradient was formed in a 260 μm-wide channel (Figure 6D). Freshly purified WT mouse neutrophils migrated robustly up the gradient. fMLF-induced chemotaxis of *Grx1*$^{-/-}$ neutrophils was severely defective, showing slow migration towards the direction of higher chemoattractant (Figure 6E–F). Compared to WT neutrophils, more *Grx1*$^{-/-}$ neutrophils stopped or slowed down during the course of chemotaxis (Figure 6G and Supplemental Movie 6). Collectively, the results demonstrate that Grx1 directly regulates chemotactic migration by modulating actin polymerization. Grx1 did not appear to be involved in directional sensing, since most neutrophils depleted of Grx1 could still migrate up the chemoattractant gradient (Figure 6E–F).

We next investigated the role of Grx1 in several other cellular processes that involve actin polymerization. We examined the morphological changes of neutrophils in response to chemoattractants. Both WT and *Grx1*$^{-/-}$ neutrophils were predominantly round before

stimulation (Figure 6H, Movies S7). When uniformly stimulated with fMLF, both WT and *Grx1*$^{-/-}$ neutrophils displayed membrane ruffles and polarized, forming distinct psudopods and uropods. We quantified the fraction of ruffling neutrophils and found that more WT neutrophils ruffled in comparison to *Grx1*$^{-/-}$ neutrophils (Figure 6I) at each time points examined.

It is known that actin is able to modulate integrin activation state directly and indirectly as the result of regulated changes in integrin-cytoskeleton linkages (Gardel et al., 2010). Thus we also examined whether disruption of Grx1 can cause defect in cell adhesion using a flow-based adhesion assay (Kasorn et al., 2009) (Figure 6J and Movies S8–9). *Grx1*$^{-/-}$ and WT mouse neutrophils were stimulated or unstimulated (as controls) with chemoattractant fMLF and then plated on fibronectin (ligand for α9β1, α4β1, αMβ2)-coated surface. Neutrophil adhesion was examined under conditions of fluid shear stress in a parallel plate flow chamber. In the absence of any extracellular stimuli, only a small percentage of cells adhered to the surface. Upon stimulation with fMLF, neutrophil adhesion was enhanced. Disruption of Grx1 significantly reduced the number of adhesion cells, indicating that glutathionylation and deglutathionylation also play a critical role in regulating actin polymerization during cell adhesion (Figure 6K).

Actin polymerization is also involved in the engulfment of bioparticles during phagocytosis. We wonder whether Grx1 disruption can affect the efficiency of neutrophil phagocytosis. To test this, we quantified the number of bio-particles engulfed by each neutrophil using an *ex vivo* phagocytosis assay (Figure 6L). After 30 min incubation at 37°C, an average of 375 mouse serum-opsonized fluorescein-conjugated Zymosan particles were engulfed by 100 WT neutrophils (phagocytic index). *Grx1*$^{-/-}$ neutrophils had a significantly reduced phagocytic index: only 250 Zymosan particles were engulfed by 100 neutrophils (Figure 6M). Reduced phagocytosis was also observed at all other time points examined. The suppressed phagocytosis was likely a result of reduced engulfment, since there was essentially no difference in the initial bacteria-binding capability between wild-type and Grx1-deficinet neutrophils (Figure 6N). A similar effect was detected when the *ex vivo* phagocytosis assay was conducted using purified mouse neutrophils and serum-opsonized pHrodo-labeled *E.coli* bio-particles, which fluoresce brightly red only in low pH of phagocytic vesicles (Figure 6O–P).

Disruption of Grx1 attenuates neutrophil recruitment and bacteria-killing capability in infected mice

The *ex vivo* experiments showed that neutrophils depleted of Grx1 displayed reduced chemotaxis efficiency. We next investigated whether this defect in chemotaxis will lead to impaired neutrophil recruitment to sites of inflammation in live mice using an acute peritoneal inflammation (peritonitis) model. Inflammation was induced by intraperitoneal injection of live *E.coli*. Very few peritoneal neutrophils (~ 4–6 × 10^4) were found in unchallenged wild-type and *Grx1*$^{-/-}$ mice. After induction of inflammatory reactions, the number of neutrophils in the wild-type peritoneal exudate reached nearly 6 × 10^6, 4 hrs after *E.coli* injection. In contrast, *Grx1*$^{-/-}$ mice showed a dramatic decrease in *E. coli* induced neutrophil recruitment - about 3 × 10^6 neutrophils were recruited to the peritoneal cavity, 4

hrs after induction (Figure 7A). To further evaluate the physiological role of Grx1 in host defense, we explored the survival rate of intraperitoneally injected live *E.coli* (Figure 7B). In wild-type (WT) mice, the number of bacteria was reduced significantly 4 hour after the challenge, reflecting the bacteria-killing capability of neutrophils. We detected more bacteria in inflamed *Grx1*$^{-/-}$ mice, suggesting that these mice have reduced bacteria-killing capability (Figure 7C). In fact, due to bacteria proliferation, the number of bacteria even increased 4 hours after the challenge. Collectively, these results support the conclusion that ROS-induced actin glutathionylation and its modulation by glutaredoxin 1 are key physiological regulatory mechanisms controlling actin dynamics in neutrophils in innate immunity and host defense.

In the *Grx1*$^{-/-}$ mice, Grx1 gene was disrupted in all cell types. Thus neutrophil recruitment in these mice could also be affected by the altered endothelial cell function. Additionally, abnormal production of cytokine from mast cells or macrophages in peritoneal cavity may affect neutrophil recruitment. To compare neutrophil recruitment under exactly the same environment, an adoptive transfer experiment was conducted (Figure 7D). We labeled *ex vivo* purified wild-type neutrophils with intracellular fluorescent dye 5-(and -6)-carboxyfluorescein diacetate succinimidyl esters (CFSE) (green) and *Grx1*$^{-/-}$ neutrophils with 5-(and -6)-chloromethyl SNARF-1 acetate (red), or vice versa. The mixed (1:1) population was intravenously injected into wild-type recipient mice 4 hour after the intraperitoneal *E. coli* injection. By doing this, variability caused by difference in inflammatory environment in each individual recipient mouse was eliminated. *Grx1*$^{-/-}$ (red) and wild-type (green) neutrophils were identified by their unique fluorescent labels (Figure 7E). Since neutrophil numbers were measured 5 hour after the *E.coli* injection, when neutrophil death is minimal, the ratio of *Grx1*$^{-/-}$ neutrophils to WT neutrophils most likely reflected their relative capability to migrate to the inflamed peritoneal cavity. Consistent with the *ex vivo* results, we detected a much reduced peritoneal recruitment of *Grx1*$^{-/-}$ neutrophils compared with wild-type neutrophils (Figure 7F). These results further demonstrated that *Grx1*$^{-/-}$ neutrophils have an intrinsic defect in the recruitment to sites of inflammation.

Discussion

Cytoplasmic actin in neutrophils continuously polymerizes and depolymerizes in an ATP-powered cycle (Pollard and Borisy, 2003). Signal-dependent regulation of actin dynamics is pivotal for a variety of cellular processes including migration, adhesion, and phagocytosis, and thus is crucial for neutrophils to fulfill their roles in innate immunity. Here we show that signal-elicited ROS production promoted actin glutathionylation and the subsequent depolymerization.

Actin is one of the major glutathionylated proteins in neutrophils undergoing respiratory burst. Chemoattractant stimulation led to an increase in actin glutathionylation. Importantly, pharmacological inhibition of oxidative burst resulted in complete inhibition of actin glutathionylation, suggesting that NADPH-oxidase mediated ROS plays a key role in eliciting actin glutathionylation. Neutrophils with inhibited ROS production formed more frequent multiple pseudopodia and showed reduced chemotaxis efficiency as they migrated

up a chemoattractant concentration gradient. We used two fluorescent dyes to show that ROS, including H_2O_2 specifically, were produced at the pseudopods of cells, where actin polymerization is known to be robust. As glutathionylated actin cannot polymerize efficiently, we propose that inhibition of ROS production abrogated actin glutathionylation and hence resulted in enhanced actin polymerization, leading to formation of exasperated multiple pseudopodia. Supporting this model, we detected elevated F-actin in ROS inhibited neutrophils. Moreover, we found that the multiple pseudopodia defect observed in ROS depleted cells could be rescued by siRNA silencing of Glutaredoxin 1 (Grx1), an enzyme that catalyzes actin deglutathionylation and thus decreases the amount of glutathionylated actin, or by Cd^{2+}, a potent inhibitor of Grx, suggesting that ROS dependent reversible actin glutathionylation plays a physiological role in regulating actin polymerization during neutrophil chemotaxis. To further establish the causal link between actin glutathionylation and pseudopod formation, we reduced actin glutathionylation by treating neutrophils with sodium arsenite, a drug that inhibits actin glutathionylation via blocking the formation of sulfenic acid intermediary, or overexpressing Grx1. Similar with the DPI treatment, sodium arsenite or Grx1 overexpression could significantly decrease actin glutathionylation in neutrophils, and consequently impair neutrophil chemotaxis and increase multiple pseudopodia formation during chemotaxis. Taken together, these results demonstrate a critical role of actin glutathionylation in neutrophil chemotaxis. In chemotaxing neutrophils, actin polymerization, ROS production, and actin glutathionylation occur sequentially. NADPH-oxidase mediated ROS production occurs after the initial actin polymerization (about 0.5–1 min after chemoattractant stimulation) and pseudopod formation. These ROS are produced (about 1–2 min after chemoattractant stimulation) and localized at pseudopods and induce modification of actin to a dysfunctional glutathionylated form. ROS-induced actin glutathionylation peaks at about 5 min after chemoattractant stimulation, leading to enhanced actin depolymerization and disassembly of pseudopods. This mechanism is critical for efficient chemotaxis. Neutrophils with reduced actin glutathionylation displayed enhanced F-actin polymerization, leading to multiple pseudopod formation and impaired chemotaxis.

Finally, using a *Grx1*$^{-/-}$ mouse, we showed that elevating actin glutathionylation by disrupting Grx1 attenuated actin polymerization, and consequently impaired neutrophil polarization, chemotaxis, adhesion, and phagocytosis. Consistent with the *ex vivo* results, *Grx1*$^{-/-}$ murine neutrophils showed impaired *in vivo* recruitment to sites of inflammation and reduced bactericidal capability. Taken together, these results demonstrate that physiologically produced ROS promote depolymerization of filamentous actin by driving reversible actin glutathionylation, and for the first time show that such a mechanism is physiologically involved in several cellular processes mediated by actin.

Glutathionylation of the critical cysteine in actin reduces the ability of G-actin to polymerize into F-actin polymers. Similar to other types of protein modification (e.g. phosphorylation), the glutathionylation is not 100%. In addition, actin glutathionylation doesn't completely inhibit actin polymerization (Dalle-Donne et al., 2003; Lassing et al., 2007; Shelton et al., 2005; Wang et al., 2001). Consistently, we could still detect F-actin in wild-type neutrophils at 5 min when actin glutathionylation peaked. However, reducing actin glutathionylation by

overexperssing Grx1 significantly increased the amount of F-actin. ROS-induced actin glutathionylation peaked at about 5 min after chemoattractant stimulation, thus we observed most significant increase in F-actin amount in Grx1 overexpressing neutrophils at this time point. In neutrophils, there are different forms of F-actin (e.g. cortical actin, stress fibres, endosome and Golgi actin, and nuclear actin)(Chhabra and Higgs, 2007). Many of them are not regulated by chemoattractant. Only chemoattractant-elicited actin polymerization is involved in pseudopodia formation during chemotaxis. In wild-type cells, the amount of F-actin goes back to the basal concentration 5 min after chemoattractant stimulation. In contrast, more than half of the chemoattractant-elicited F-actin remained in Grx1 overexpressing cells.

Experimental Procedures

Mice

Grx1$^{-/-}$ mice were kindly provided by Dr. Y.S.Ho and were backcrossed more than 14 generations onto a : C57BL/6 background (Ho et al., 2007). X-linked CGD mice (Pollock et al., 1995) that contain disrupted alleles of the gene encoding gp91^{phox} (B6.129S6-Cybbtm1Din/J, Strain: C57BL/6) were purchased from the Jackson Laboratories (Bar Harbor, ME). In all the experiments performed, we used age-matched C57BL/6 mice as wild-type controls. All procedures involving mice were approved and monitored by the Children's Hospital Animal Care and Use Committee.

BioGEE Treatment and Immunoprecipitation

Human Neutrophils (10^7 cells) were incubated with 250 μM Biotynylated glutathione ester (BioGEE, Molecular Probes) for 1 hr at 37°C in HBSS containing 5mM Diisopropylfluorophosphate (DFP, Calbiochem). Neutrophils were then stimulated with 100 nM fMLF for 5 min, and then lysed directly in ice cold RIPA buffer (50 mM Tris-HCl, 150 mM NaCl, 2 mM EDTA, 1% Triton-X, pH 7.4) containing Protease Inhibitor cocktail (Roche), 1 mM DFP and 1 mM PMSF. Actin (Millipore) or Ask1 (Cell Signaling) antibody was then added to equal portions of the lysate along with Protein A/G beads and mixed for 1 hr at 4°C. The beads were then washed 3× in RIPA buffer and bound protein was eluted by boiling in 2× LDS buffer containing 5% β-Mercaptoethanol. Immunoprecipitated protein was then resolved and probed for protein glutathionylation using Streptavidin-HRP (1:1000) or actin, using an actin antibody (Cytoskeleton Inc.) and Clean-IP detection kit (Pierce). Alternatively, Streptavidin-agarose pull down was performed using BioGEE treated or untreated neutrophil lysates, as described earlier (Clavreul et al., 2006).

Glutathionylation Immunostaining

Human neutrophils (0.3×10^6) in HBSS with 0.1% BSA were stimulated with 25 nM fMLF and plated onto glass coverslips for 5 mins. Neutrophils were then fixed with ice cold methanol/acetone (50%–50%) containing 100 mM NEM for 5mins, washed twice with PBS plus 100 mM NEM for 5 min each to remove free glutathione from the cells and then fixed with 4% formaldehyde in PBS plus 100 mM NEM for 10 min. After three washes with PBS/100 mM NEM, neutrophils were permeabilized with 0.2% Triton-X in PBS plus 100 mM NEM, blocked with PBS plus 25 mM NEM (PBS/NEM) for 30mins at 4°C and then

preblocked with PBS/NEM/2% BSA blocking buffer for 30mins at RT. Primary antibodies (1:500, Mouse GSH (Virogen) and 1:200, rabbit actin (Sigma)) were then added to the fixed cells in the blocking buffer for 1 hour, washed three times with PBS/NEM, followed by incubation with secondary antibodies (1:1000, anti-mouse IgG, anti-rabbit IgG, Molecular Probes) for 30 min and three washes with PBS/NEM. For DTT treatment, NEM in all steps after Triton-X permeabilization was replaced with 10 mM DTT.

Assays for neutrophil functions

Some related assays, including quantification of F-actin by phalloidin labeling, measurement of superoxide production by luminol chemiluminescence, micropipette chemotaxis assay, culturing and differentiation of HL60 cells, and Wright-Giemsa staining were described in previous publications (Hattori et al., 2007; Prasad et al., 2011; Subramanian et al., 2007). Other methods, such as neutrophil isolation, glutathionylation immunoblotting, labeling and imaging of ROS, EZ-taxiscan chemotaxis assay, neutrophil adhesion under shear flow, analysis of cell tracks and morphology, polarization assay, siRNA silencing of glutaredoxin, generation of Grx1-overexpressing HL-60 cells using lentivirus, phagocytosis assay, peritonitis model, *in vivo* bacteria killing, and neutrophil adoptive transfer were described in the Supplemental Experimental Procedures.

Statistics

Analysis of statistical significance for indicated data sets was performed using the Student's *t* test capability on Microsoft Excel.

Supplementary Material

Refer to Web version on PubMed Central for supplementary material.

Acknowledgments

The authors thank Leslie Silberstein, John Manis, and Li Chai for helpful discussions. Dr. Yvonne Janssen-Heininger (The University of Vermont) for preparing and sending the *Grx1*$^{-/-}$ mice. H. Luo is supported by NIH grants HL085100 and GM076084. C.J. Chang is supported by NIH GM 79465 and is an investigator with the Howard Hughes Medical Institute.

References

Aesif SW, Anathy V, Kuipers I, Guala AS, Reiss JN, Ho YS, Janssen-Heininger YM. Ablation of glutaredoxin-1 attenuates lipopolysaccharide-induced lung inflammation and alveolar macrophage activation. Am J Respir Cell Mol Biol. 2011; 44:491–499. [PubMed: 20539014]

Chhabra ES, Higgs HN. The many faces of actin: matching assembly factors with cellular structures. Nat Cell Biol. 2007; 9:1110–1121. [PubMed: 17909522]

Chrestensen CA, Starke DW, Mieyal JJ. Acute cadmium exposure inactivates thioltransferase (Glutaredoxin), inhibits intracellular reduction of protein-glutathionyl-mixed disulfides, and initiates apoptosis. J Biol Chem. 2000; 275:26556–26565. [PubMed: 10854441]

Chung S, Sundar IK, Yao H, Ho YS, Rahman I. Glutaredoxin 1 regulates cigarette smoke-mediated lung inflammation through differential modulation of I{kappa}B kinases in mice: impact on histone acetylation. Am J Physiol Lung Cell Mol Physiol. 2010; 299:L192–L203. [PubMed: 20472709]

Clavreul N, Bachschmid MM, Hou X, Shi C, Idrizovic A, Ido Y, Pimentel D, Cohen RA. S-glutathiolation of p21ras by peroxynitrite mediates endothelial insulin resistance caused by oxidized low-density lipoprotein. Arterioscler Thromb Vasc Biol. 2006; 26:2454–2461. [PubMed: 16931794]

Dalle-Donne I, Giustarini D, Rossi R, Colombo R, Milzani A. Reversible S-glutathionylation of Cys 374 regulates actin filament formation by inducing structural changes in the actin molecule. Free Radic Biol Med. 2003; 34:23–32. [PubMed: 12498976]

Dickinson BC, Chang CJ. Chemistry and biology of reactive oxygen species in signaling or stress responses. Nat Chem Biol. 2011; 7:504–511. [PubMed: 21769097]

Dickinson BC, Peltier J, Stone D, Schaffer DV, Chang CJ. Nox2 redox signaling maintains essential cell populations in the brain. Nat Chem Biol. 2011; 7:106–112. [PubMed: 21186346]

Dinauer MC. Chronic granulomatous disease and other disorders of phagocyte function. Hematology Am Soc Hematol Educ Program. 2005:89–95. [PubMed: 16304364]

Gallogly MM, Mieyal JJ. Mechanisms of reversible protein glutathionylation in redox signaling and oxidative stress. Curr Opin Pharmacol. 2007; 7:381–391. [PubMed: 17662654]

Gardel ML, Schneider IC, Aratyn-Schaus Y, Waterman CM. Mechanical integration of actin and adhesion dynamics in cell migration. Annu Rev Cell Dev Biol. 2010; 26:315–333. [PubMed: 19575647]

Ghezzi P. Regulation of protein function by glutathionylation. Free Radic Res. 2005; 39:573–580. [PubMed: 16036334]

Hattori H, Subramanian KK, Sakai J, Jia Y, Li Y, Porter TF, Loison F, Sarraj B, Kasorn A, Jo H, et al. Small-molecule screen identifies reactive oxygen species as key regulators of neutrophil chemotaxis. Proc Natl Acad Sci U S A. 2010; 107:3546–3551. [PubMed: 20142487]

Hattori H, Zhang X, Jia Y, Subramanian KK, Jo H, Loison F, Newburger PE, Luo HR. RNAi screen identifies UBE2D3 as a mediator of all-trans retinoic acid-induced cell growth arrest in human acute promyelocytic NB4 cells. Blood. 2007; 110:640–650. [PubMed: 17420285]

Ho YS, Xiong Y, Ho DS, Gao J, Chua BH, Pai H, Mieyal JJ. Targeted disruption of the glutaredoxin 1 gene does not sensitize adult mice to tissue injury induced by ischemia/reperfusion and hyperoxia. Free Radic Biol Med. 2007; 43:1299–1312. [PubMed: 17893043]

Hurd TR, Costa NJ, Dahm CC, Beer SM, Brown SE, Filipovska A, Murphy MP. Glutathionylation of mitochondrial proteins. Antioxid Redox Signal. 2005; 7:999–1010. [PubMed: 15998254]

Janssen-Heininger YM, Mossman BT, Heintz NH, Forman HJ, Kalyanaraman B, Finkel T, Stamler JS, Rhee SG, van der Vliet A. Redox-based regulation of signal transduction: principles, pitfalls, and promises. Free Radic Biol Med. 2008; 45:1–17. [PubMed: 18423411]

Johansson M, Lundberg M. Glutathionylation of beta-actin via a cysteinyl sulfenic acid intermediary. BMC Biochem. 2007; 8:26. [PubMed: 18070357]

Kasorn A, Alcaide P, Jia Y, Subramanian KK, Sarraj B, Li Y, Loison F, Hattori H, Silberstein LE, Luscinskas WF, et al. Focal adhesion kinase regulates pathogen-killing capability and life span of neutrophils via mediating both adhesion-dependent and - independent cellular signals. J Immunol. 2009; 183:1032–1043. [PubMed: 19561112]

Kim SO, Merchant K, Nudelman R, Beyer WF Jr, Keng T, DeAngelo J, Hausladen A, Stamler JS. OxyR: a molecular code for redox-related signaling. Cell. 2002; 109:383–396. [PubMed: 12015987]

Lassing I, Schmitzberger F, Bjornstedt M, Holmgren A, Nordlund P, Schutt CE, Lindberg U. Molecular and structural basis for redox regulation of beta-actin. J Mol Biol. 2007; 370:331–348. [PubMed: 17521670]

Leichert LI, Jakob U. Global methods to monitor the thiol-disulfide state of proteins in vivo. Antioxid Redox Signal. 2006; 8:763–772. [PubMed: 16771668]

Lofgren S, Fernando MR, Xing KY, Wang Y, Kuszynski CA, Ho YS, Lou MF. Effect of thioltransferase (glutaredoxin) deletion on cellular sensitivity to oxidative stress and cell proliferation in lens epithelial cells of thioltransferase knockout mouse. Invest Ophthalmol Vis Sci. 2008; 49:4497–4505. [PubMed: 18586881]

Meyer Y, Buchanan BB, Vignols F, Reichheld JP. Thioredoxins and glutaredoxins: unifying elements in redox biology. Annu Rev Genet. 2009; 43:335–367. [PubMed: 19691428]

Miller EW, Dickinson BC, Chang CJ. Aquaporin-3 mediates hydrogen peroxide uptake to regulate downstream intracellular signaling. Proc Natl Acad Sci U S A. 2010; 107:15681–15686. [PubMed: 20724658]

Pollard TD, Borisy GG. Cellular motility driven by assembly and disassembly of actin filaments. Cell. 2003; 112:453–465. [PubMed: 12600310]

Pollock JD, Williams DA, Gifford MA, Li LL, Du X, Fisherman J, Orkin SH, Doerschuk CM, Dinauer MC. Mouse model of X-linked chronic granulomatous disease, an inherited defect in phagocyte superoxide production. Nat Genet. 1995; 9:202–209. [PubMed: 7719350]

Prasad A, Jia Y, Chakraborty A, Li Y, Jain SK, Zhong J, Roy SG, Loison F, Mondal S, Sakai J, et al. Inositol hexakisphosphate kinase 1 regulates neutrophil function in innate immunity by inhibiting phosphatidylinositol-(3,4,5)-trisphosphate signaling. Nat Immunol. 2011; 12:752–760. [PubMed: 21685907]

Saurin AT, Neubert H, Brennan JP, Eaton P. Widespread sulfenic acid formation in tissues in response to hydrogen peroxide. Proc Natl Acad Sci U S A. 2004; 101:17982–17987. [PubMed: 15604151]

Shelton MD, Chock PB, Mieyal JJ. Glutaredoxin: role in reversible protein s-glutathionylation and regulation of redox signal transduction and protein translocation. Antioxid Redox Signal. 2005; 7:348–366. [PubMed: 15706083]

Subramanian KK, Jia Y, Zhu D, Simms BT, Jo H, Hattori H, You J, Mizgerd JP, Luo HR. Tumor suppressor PTEN is a physiologic suppressor of chemoattractant-mediated neutrophil functions. Blood. 2007; 109:4028–4037. [PubMed: 17202315]

Subramanian, KK.; Luo, HR. Non-classical roles of NADPH-oxidase dependent Reactive Oxygen Species in Phagocytes. In: Kohlund, RHaS, editor. Granulocytes: Classification, Toxic Materials Produced and Pathology. Nova Science Publishers, Inc.; 2009.

Tsapara A, Kardassis D, Moustakas A, Gravanis A, Stournaras C. Expression and characterization of Cys374 mutated human beta-actin in two different mammalian cell lines: impaired microfilament organization and stability. FEBS Lett. 1999; 455:117–122. [PubMed: 10428484]

Wang J, Boja ES, Tan W, Tekle E, Fales HM, English S, Mieyal JJ, Chock PB. Reversible glutathionylation regulates actin polymerization in A431 cells. J Biol Chem. 2001; 276:47763–47766. [PubMed: 11684673]

Ying J, Clavreul N, Sethuraman M, Adachi T, Cohen RA. Thiol oxidation in signaling and response to stress: detection and quantification of physiological and pathophysiological thiol modifications. Free Radic Biol Med. 2007; 43:1099–1108. [PubMed: 17854705]

Highlights

- Chemoattractant-elicited ROS lead to elevated actin glutathionylation.
- ROS negatively regulate actin polymerization by driving actin glutathionylation.
- ROS-induced actin glutathionylation is tightly regulated by Grx1.
- Disruption of Grx1 impairs neutrophil recruitment and bactericidal capability in vivo.

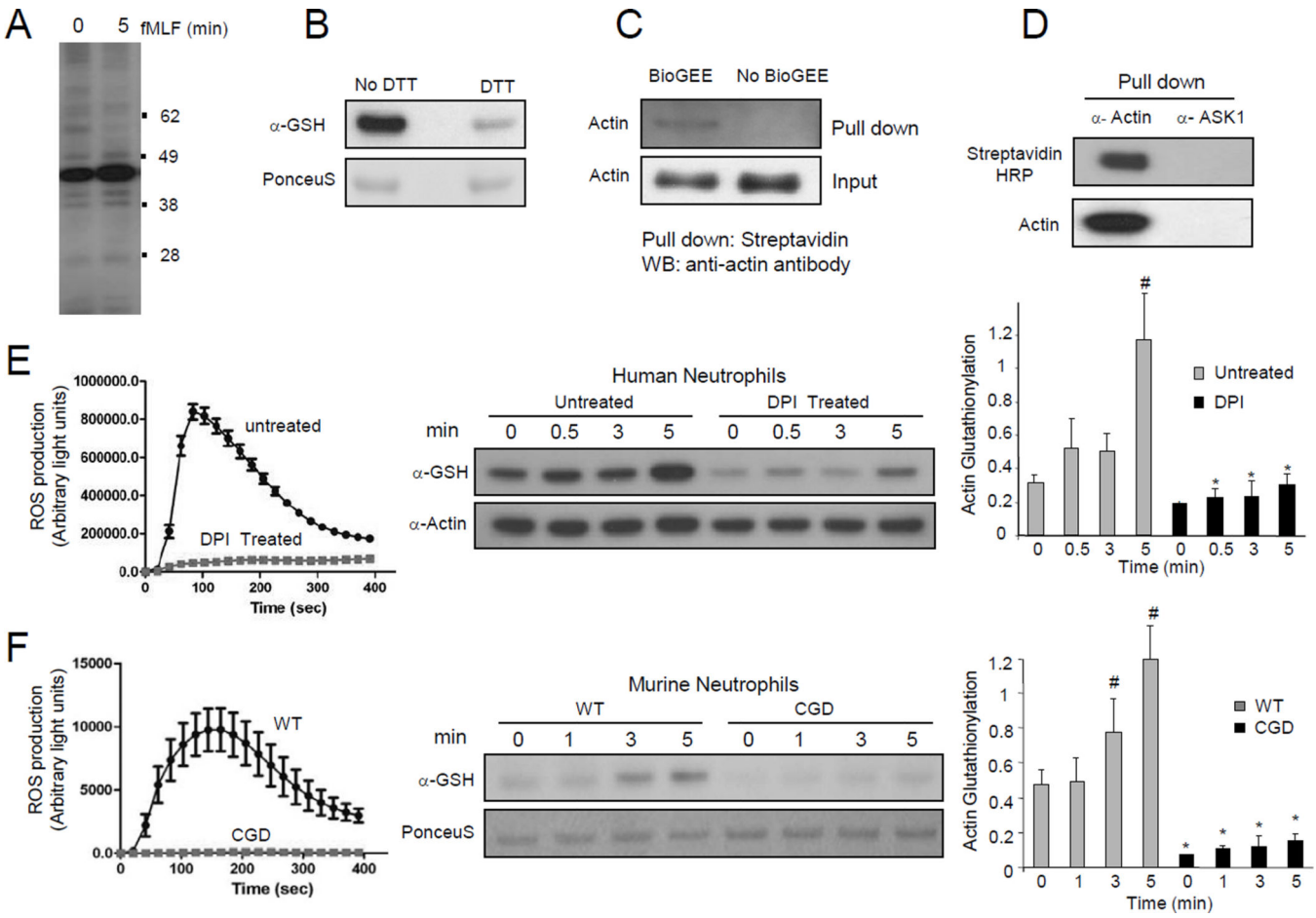

Figure 1. NADPH oxidase-mediated ROS production induced actin glutathionylation in chemoattractant-stimulated neutrophils

(A) Protein glutathionylation in chemoattractant-stimulated human neutrophils. **(B)** Treatment with DTT leads to reduction of glutathione mixed disulfides. **(C)** Biotinylated glutathione (BioGEE)-modified proteins were pulled down from neutrophil lysates using Streptavidin agarose beads and probed with a β-actin antibody. **(D)** Actin was immunoprecipitated from BioGEE labeled neutrophil lysates (5 min after fMLF stimulation) and probed for Biotinylated-glutathione modification using Streptavidin-HRP. ASK1, a cytosolic protein, was used as a negative control. **(E)** Actin glutathionylation in fMLF-stimulated human neutrophils is dependent on NADPH oxidase activation. Human neutrophils pretreated with 50 μM DPI for 30 min were stimulated with 100 nM fMLF. Ratio of glutathionylated-actin to total actin is reported as actin-glutathionylation in the bar-graph (*right*). ROS production was evaluated by monitoring chemiluminescence (*left*). **(F)** Actin glutathionylation in fMLF-stimulated murine neutrophils stimulated with 1 μM fMLF. Data represents mean±SD from n=3 wells from one experiment representative of three. *, $p < 0.001$, versus WT. #, $p < 0.001$ versus time 0.

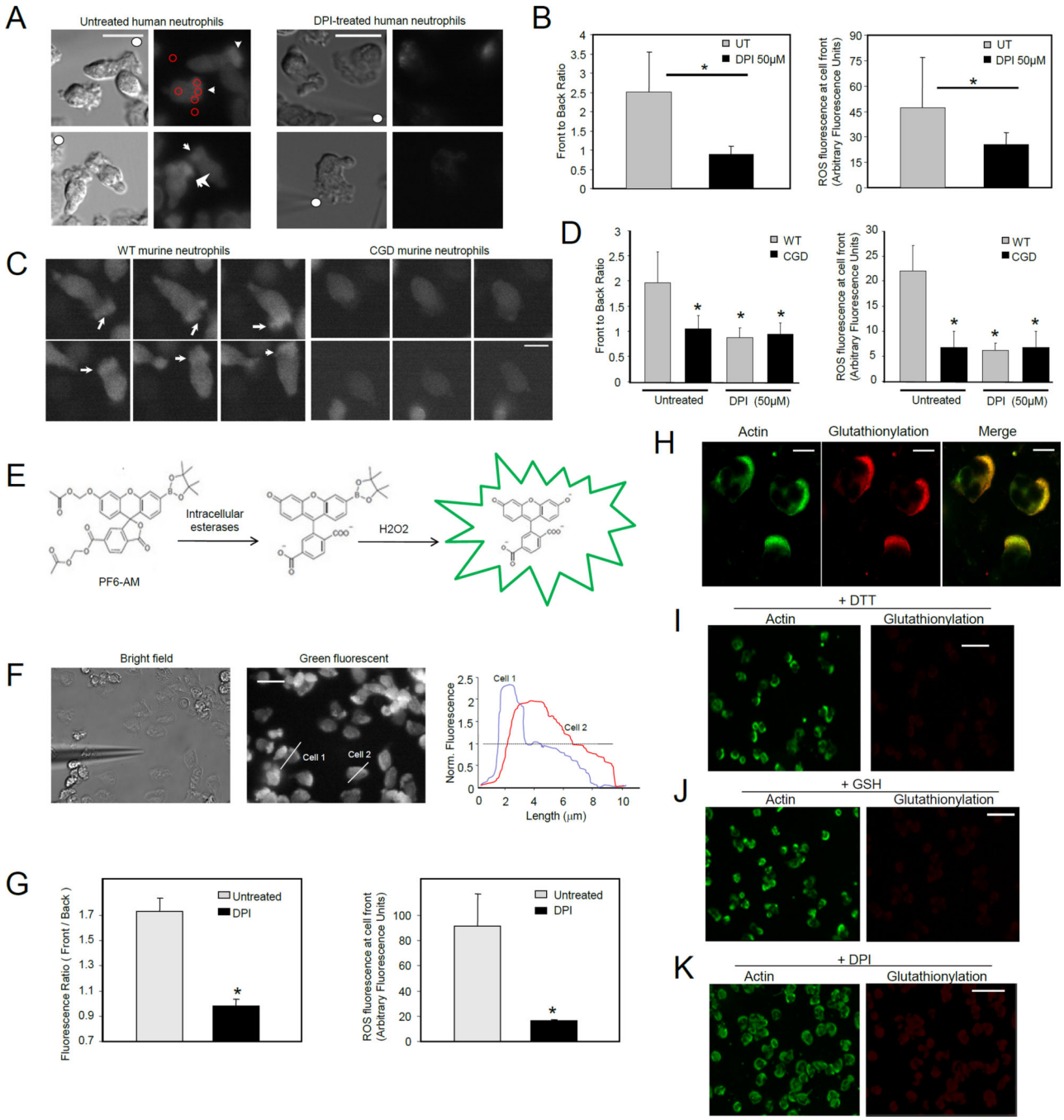

Figure 2. Both NADPH oxidase-mediated ROS production and protein glutathionylation occurred at pseudopodia of migrating human neutrophils, colocalizing with actin

(A) Human neutrophils were labeled with ROS dye CM-H2DCFDA and exposed to a micropipette tip filled with 1 μM fMLF (denoted by solid white circle). Leading edges of migrating cells were marked by white arrows. Scale bars represent 10 μm. **(B)** Quantification of NADPH oxidase-dependent ROS localization at the front of migrating neutrophils. Four to five regions of interest (ROIs, red circles in Figure 2A) were randomly drawn at the front and back of the cell, as well as background regions of the image. Data are

represented as mean±SD from n=12 cells. *, $p < 0.001$, versus untreated neutrophils. **(C)** Murine bone marrow neutrophils were labeled with 1 CM-H2DCFDA and exposed to a uniform bolus of chemoattractant (50 nM fMLF). Fluorescence images show randomly migrating neutrophils in three consecutive frames with 15 sec interval. Arrow heads point towards ROS localization at pseudopodia. Scale bars represent 5 μm. **(D)** Front to back ratio and ROS fluorescence intensity at the front of the untreated or DPI treated WT or CGD neutrophils were measured as described above. Data are represented as mean±SD from n=10 cells. *, $p < 0.001$, versus untreated WT neutrophils. **(E)** Mechanism of selective detection of intracellular H_2O_2 by PF6-AM. **(F)** Subcellular localization of H_2O_2 in chemotaxing neutrophils in a fMLF gradient. Human neutrophils were labeled with 1 μM of PF6-AM. Fluorescence intensity was measured by scanning a line (white line) through a cell with IPLab software. Shown are profiles of two representative cells. In this experiment, chemotactic gradient was generated with a micropipette filled with 10 μM fMLF. Scale bars represent 10 μm. **(G)** Front to back ratio and ROS fluorescence intensity at the front of the cell were calculated from images of untreated and 50 μM DPI-treated cells. Data are represented as mean±SD from n=15 cells. *, $p<10^{-5}$ versus untreated neutrophils. **(H)** Distribution of glutathionylation and actin in fMLF-stimulated human neutrophils. Scale bars represent 5 μm. **(I)** Glutathionylation staining was conducted in the presence of 10 mM DTT. **(J)** Addition of excess amount of reduced GSH to primary antibody mix abrogated glutathionylation localization at the leading edge but did not affect detection of actin localization using the actin antibody. **(K)** Neutrophils were treated with 50 μM DPI before the fMLF stimulation. Glutathionylation staining was conducted as described in (H). The scale bars in I–K represent 20 μm.

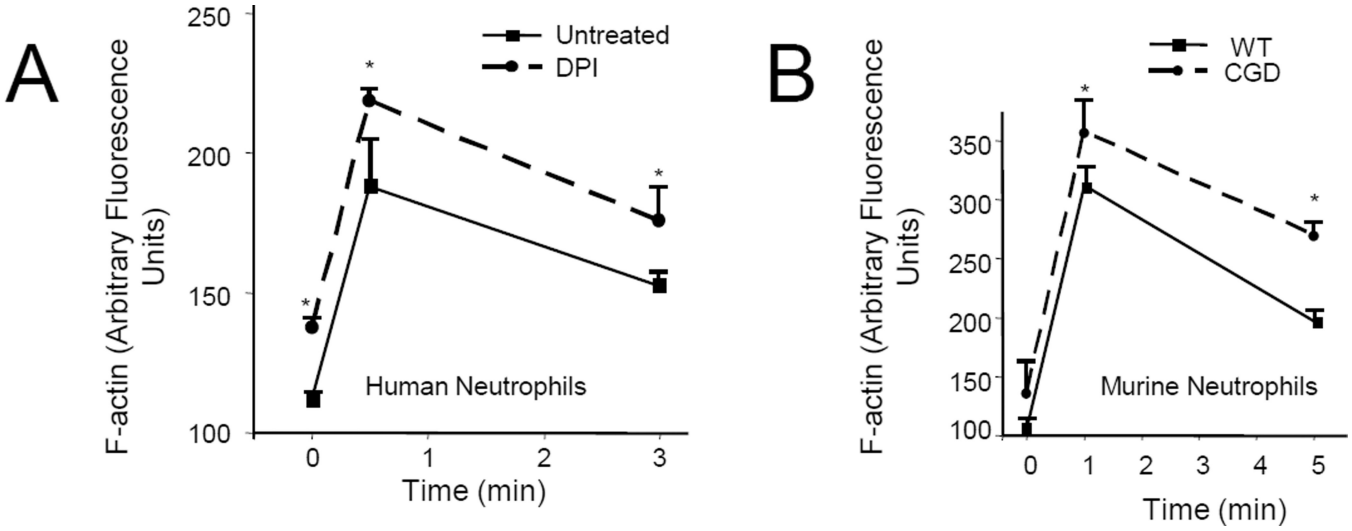

Figure 3. Suppression of NADPH oxidase-mediated ROS production led to elevated actin polymerization in neutrophils

(A) Actin polymerization in human neutrophils treated with (or without) DPI. **(B)** Actin polymerization in WT and CGD murine neutrophils. Results are the means (±SD) of three independent experiments. *$p < 0.01$ versus WT neutrophils (Student's t test).

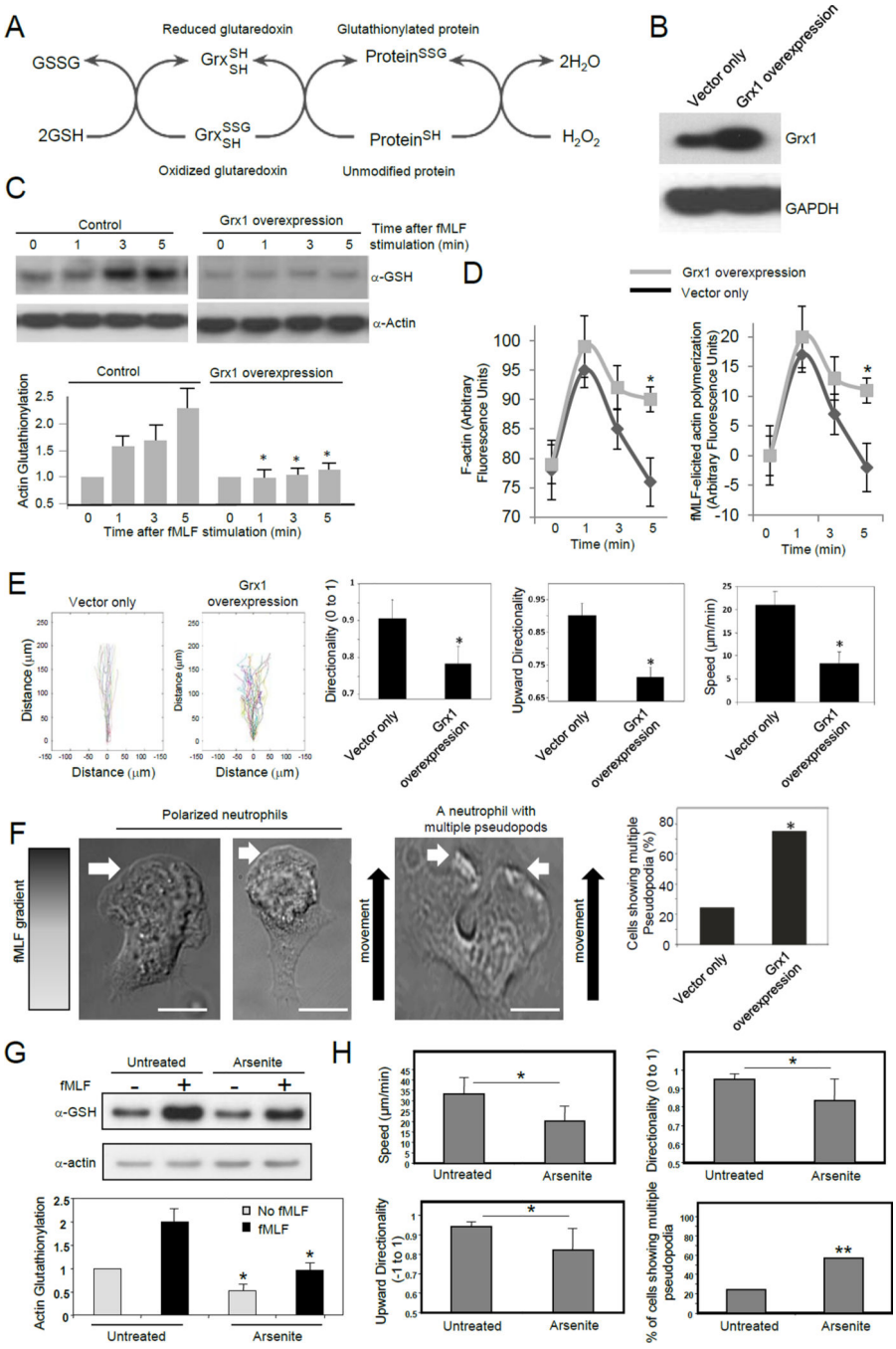

Figure 4. Reducing actin glutathionylation led to increased F-actin, formation of multiple pseudopods, and defective chemotaxis

(A) Actin glutathionylation is a dynamic reversible process that can be regulated by glutaredoxin. **(B)** Overexpression of Grx1 in neutrophil like differentiated HL60 cells. **(C)** Grx1 overexpression reduced actin glutathionylation. Data represents means ± SD of three experiments. * $p<0.01$ versus the control. **(D)** Grx1 overexpression augmented the amount of F-actin. fMLF-elicited actin polymerization was calculated as the increase of F-actin amount compared to time 0. Data shown are means ± SD of five experiments. * $p<0.01$

versus the control (vector only). **(E)** Cells overexpressing Grx1 displayed defective chemotaxis. Data are represented as mean±SD for n=20 cells, * $p<0.05$ versus control neutrophils. **(F)** Cells overexpressing Grx1 displayed multiple pseudopodia. The multiple pseudopodia was identified during cell chemotaxis in the EZ-taxiscan device. Scale bars represent 5 μm. **(G)** Sodium arsenite treatment inhibits actin glutathionylation in human neutrophils. Human neutrophils pretreated with (or without) 50 μM sodium arsenite for 30 min were stimulated with 100 nM fMLF for 5 min. * $p<0.05$ versus untreated neutrophils. **(H)** Effect of sodium arsenite treatment on human neutrophil chemotaxis. Neutrophils were evaluated for migration speed, directionality, upward directionality (n=16 cells, *, $p<0.0005$ by Student's t-test), and percentage of multiple pseudopodia (n>30 cells, **, $p<0.05$, Fisher's exact test, 2-tail).

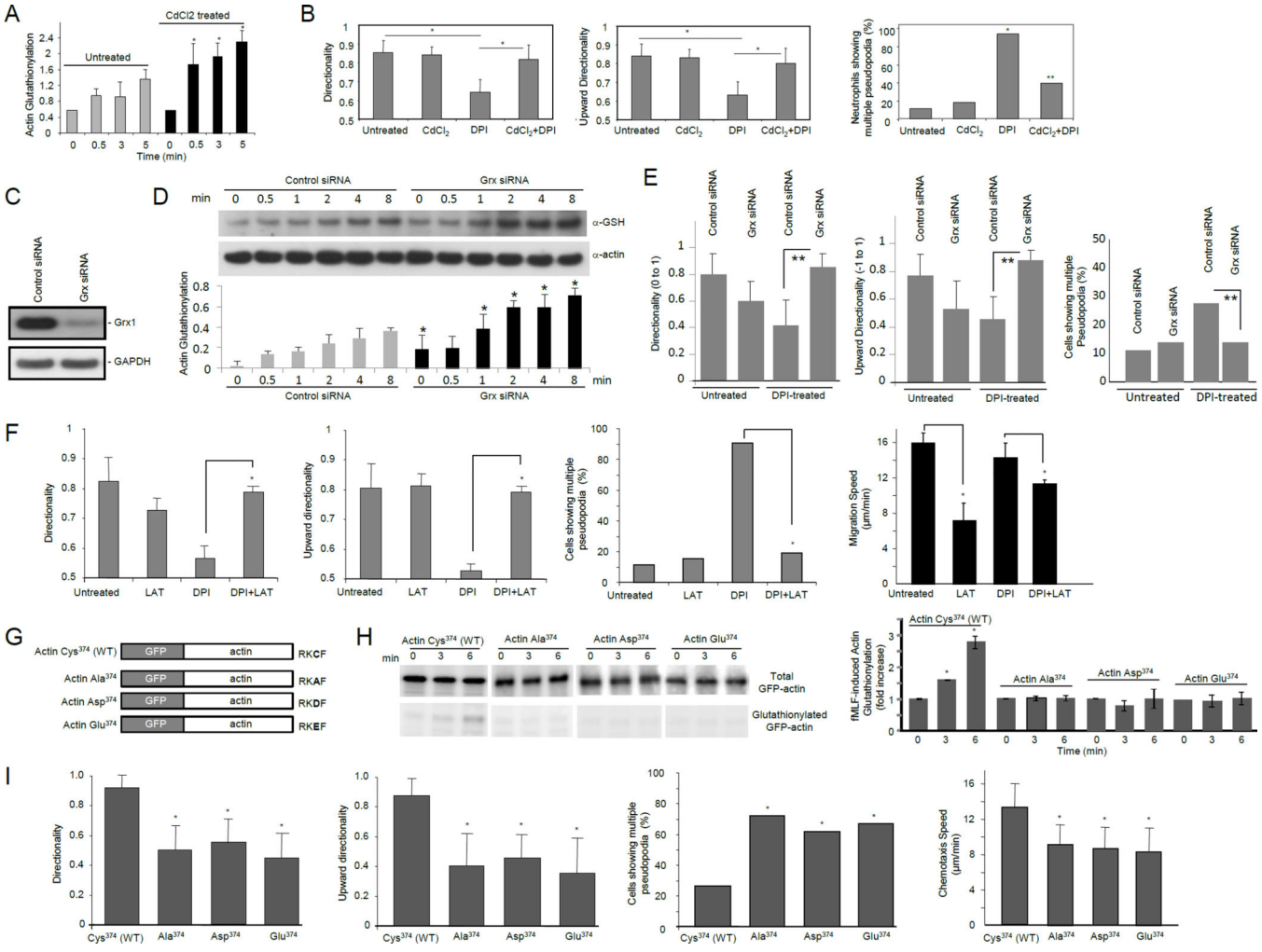

Figure 5. Neutrophil chemotaxis defects induced by ROS depletion could be rescued by inhibiting glutaredoxin

(A) Actin glutathionylation was augmented in cells treated with $CdCl_2$. Data represents means ± SD of three experiments. *, $p<0.01$ versus untreated dHL60 cells. **(B)** Augmenting protein glutathionylation by $CdCl_2$ rescued DPI-induced chemotaxis defect. Neutrophils chemotaxis was analyzed as described in Figure 4E. *, $p<0.05$ versus untreated neutrophils; *, $p<0.05$ versus DPI treated neutrophils. **(C)** siRNA silencing of Grx1 in differentiated HL60 cells. **(D)** Actin glutathionylation was enhanced in cells transfected with glutaredoxin siRNA. Data represents means ± SD of three experiments. *, $p<0.01$ versus dHL60 cells transfected with control siRNA. **(E)** siRNA silencing of glutaredoxin rescued DPI-induced chemotaxis defect. **, $p<0.005$ versus dHL60 cells transfected with control siRNA. **(F)** ROS depletion-induced formation of multiple pseudopodia and impaired directional migration were partially rescued by treatment with latrauculin B. Mouse neutrophils were pretreated with 50 μM DPI, 5 nM latrauculin B (LAT), 5 nM LAT + 2 μM $CdCl_2$, or left untreated, and then exposed to a chemoattractant gradient generated by addition of 100 nM fMLF (1 μl) in the EZ-taxiscan device. *, $p<0.005$. **(G)** Schematic representation of wild-type and mutant forms of human β-actin fused with GFP. **(H)** Cys^{374} is critical for ROS-

elicited actin glutathionylation. dHL60 cells overexpressing indicated protein were stimulated with 1μM fMLF. Overexpression of wild-type and mutant forms of GFP-actin was confirmed by western blotting with a GFP antibody. Ratio of glutathionylated GFP-actin to total GFP-actin was calculated as actin-glutathionylation. Shown in the bar-graph are the fold increases of actin-glutathionylation compared to unstimulated cells (time 0). Data represents means ± SD of three experiments. *, $p<0.01$ versus unstimulated cells. **(I)** Glutathionylation at actin-Cys^{374} is a key regulatory mechanism for efficient neutrophil chemotactic migration. Cells overexpressing EGFP-actin were identified by their higher fluorescent intensity compared with untransfected cells. The chemotaxis of transfected dHL60 cells was analyzed using an EZ-taxiscan device as described above ($n>20$ cells; *, $p<0.005$ versus dHL60 cells expressing wild-type actin).

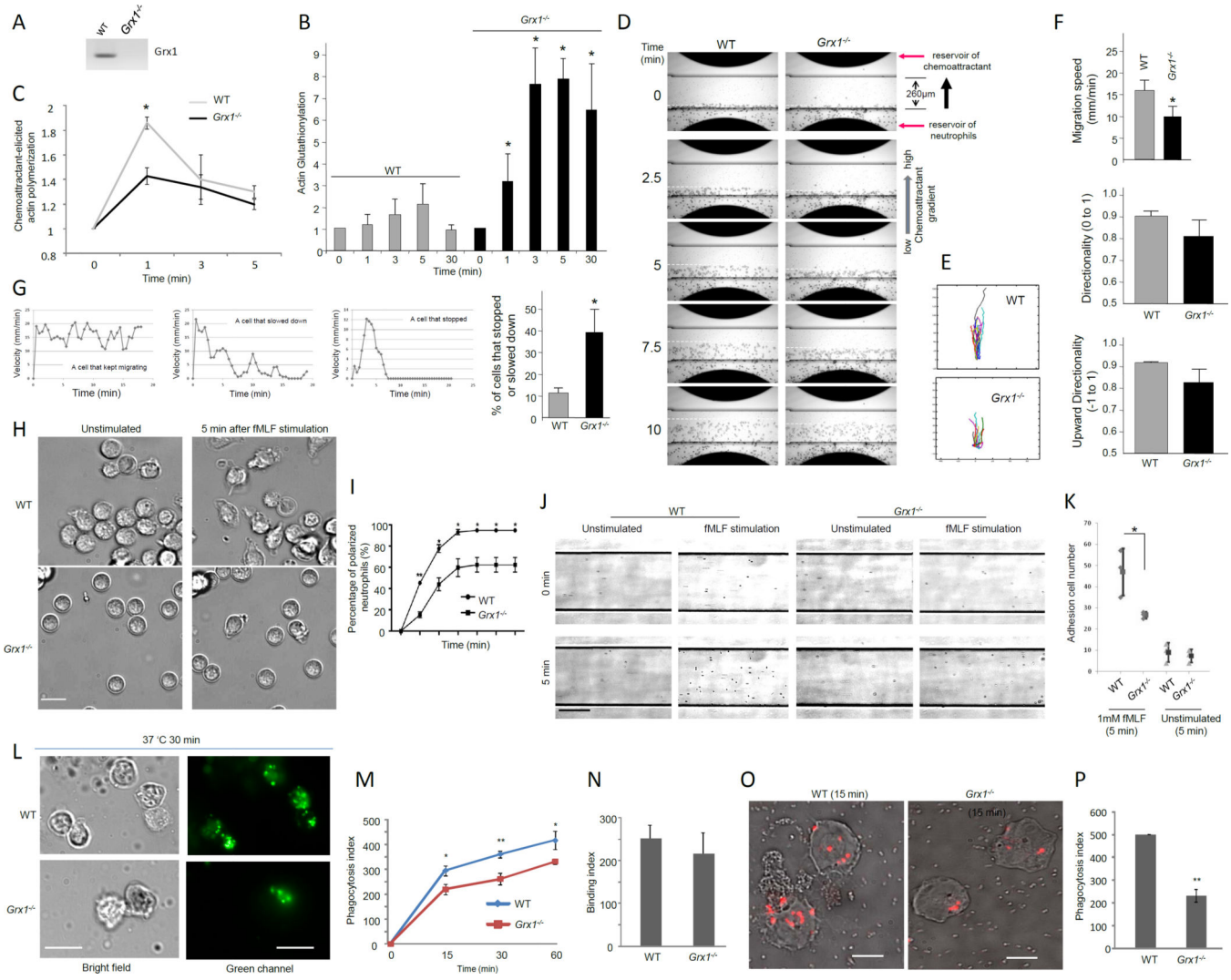

Figure 6. Disruption of glutaredoxin resulted in reduced actin polymerization and impaired neutrophil migration, polarization, adhesion, and phagocytosis

(A) Grx1 protein expression was completely abolished in neutrophils isolated from *Grx1*$^{-/-}$ mice. **(B)** Glutaredoxin disruption resulted in increased amount of glutathionylated actin in neutrophils. **(C)** Disruption of Grx1 reduced actin polymerization. **(D)** Chemotaxis of mouse neutrophils in response to chemoattractant fMLF. **(E)** Cell tracks of migrating neutrophils (cells that move at least 65 μm from the bottom of the channel) (*n=20*). **(F)** Disruption of Grx1 reduced the efficiency of neutrophil chemotaxis. * p<0.05. **(G)** The percentage of cells that stopped or slowed down during chemotaxis. * p<0.0001 versus WT neutrophils. **(H)** Chemoattractant-induced ruffling in WT and *Grx1*$^{-/-}$ neutrophils. Scale bar represents 10 μm. **(I)** The percentage of polarized neutrophils (cells that ruffled or extended pseudopods) was calculated at indicated time after fMLF stimulation. Data shown are mean ± SD collected from (*n*=3) separate preparations of neutrophils. *, *P*<0.01 versus WT neutrophils. ** p<0.0001 versus WT neutrophils. **(J)** Adhesion of WT and *Grx1*$^{-/-}$ neutrophils on fibronectin-coated flow chambers in response to fMLF stimulation. Scale bar represents 50 μm. **(K)** Grx1 disruption reduced fMLF induced cell adhesion on fibronectin-coated flow

chambers. * p<0.001 versus WT neutrophils. (**L**) *In vitro* phagocytosis assay. FITC-labeled Zymosan A bioparticles were opsonized with mouse serum and incubated with neutrophils at 37°C for indicated time. Extracellular fluorescence was quenched by trypan blue. The results shown are representative of three experiments. **(M)** Phagocytosis index (PI) was expressed as the number of bioparticles engulfed by 100 neutrophils. **(N)** Binding index was expressed as the number of bioparticles bound to 100 neutrophils (4°C for 30 min). (**O–P**) *In vitro* phagocytosis assay using pHrodo labeled E.coli bioparticles. Results are the means (±SD) of three independent experiments. *p < 0.01 versus WT neutrophils (Student's t test). Scale bars in L represent 10 μm. Scale bars in O represent 5 μm.

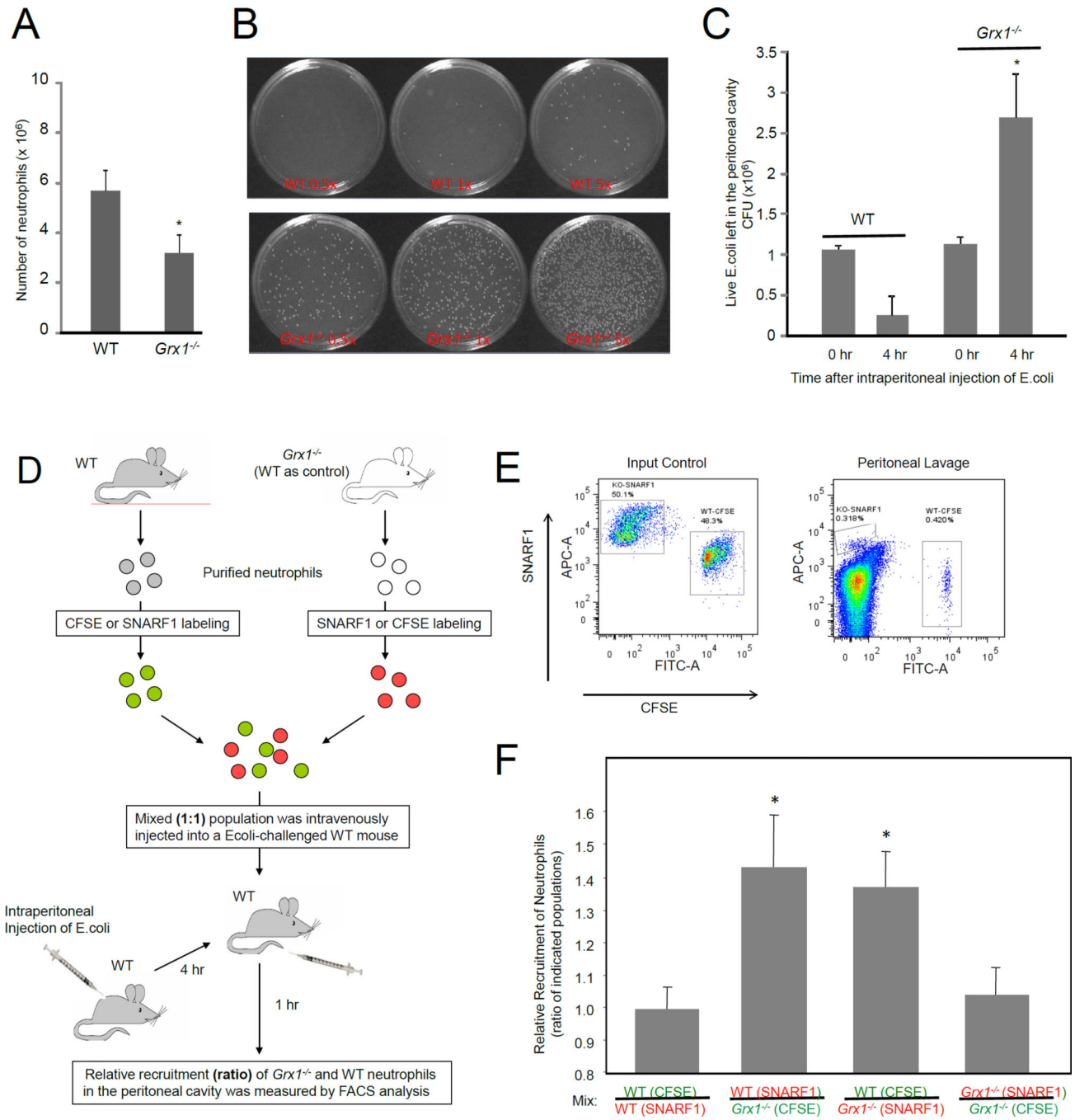

Figure 7. Disruption of Grx1 led to reduced neutrophil recruitment and impaired bacterial killing

(A) Disruption of Grx1 led to reduced neutrophil accumulation in the inflamed peritoneal cavity. Data shown are mean ± SD of *n*=3 mice. *p < 0.01 by Student's t test. **(B)** Disruption of Grx1 led to impaired bacterial killing. Images of representative culture plates are shown. **(C)** Total numbers of survived *E.coli* in the inflamed peritoneal cavity. Data are means ± SD of 4 independent experiments. *p < 0.01 versus WT mice by Student's t test. **(D)** Schematic diagram of neutrophil adoptive transfer assay. Bone marrow neutrophils from WT and

Grx1$^{-/-}$ mice were labeled with different colors (SNARF1 or CFSE labeled), mixed 1:1 and then intravenously injected into WT recipient mice that have been challenged with E.coli (intraperitoneally injected). The relative recruitment of *Grx1*$^{-/-}$ and WT neutrophils in the WT recipient was evaluated 60 min after the challenge. **(E)** The amount of adoptively transferred neutrophils recruited to the peritoneal cavity. Shown are representative FACS plots of an input control (left) and a mouse transplanted with labeled neutrophils (right). The double negative cells are the unlabeled endogenous cells. **(F)** Relative recruitment of neutrophil was calculated as the ratio of indicated populations in the peritoneal cavity. Results are the means (±SD) of three independent experiments. *, $p < 0.01$ versus WT neutrophils (Student's t test).